ADVANCED FUNCTIONAL MATERIALS
www.afm-journal.de

Polylactide-*block*-Polypeptide-*block*-Polylactide Copolymer Nanoparticles with Tunable Cleavage and Controlled Drug Release

Robert Dorresteijn, Nils Billecke, Mischa Schwendy, Sabine Pütz, Mischa Bonn, Sapun H. Parekh, Markus Klapper,* and Klaus Müllen*

A versatile nanoparticle system is presented in which drug release is triggered by enzymatic polymer cleavage, resulting in a physicochemical change of the carrier. The polylactide-*block*-peptide-*block*-polylactide triblock copolymer is generated by initiation of the ring-opening polymerization of L-lactide with a complex bifunctional peptide having an enzymatic recognition and cleavage site (Pro-Leu-Gly-Leu-Ala-Gly). This triblock copolymer is specifically bisected by matrix metalloproteinase-2 (MMP-2), an enzyme overexpressed in tumor tissues. Triblock copolymer nanoparticles formed by nonaqueous emulsion polymerization are readily transferred into aqueous media without aggregation, even in the presence of blood serum. Cleavage of the triblock copolymer leads to a significant decrease of the glass transition temperature (T_g) from 39 °C to 31 °C, likely mediating cargo release under physiological conditions. Selective drug targeting is demonstrated by hampered mitosis and increased cell death resulting from drug release via MMP-2 specific cleavage of triblock copolymer carrier. On the contrary, nanocarriers having a scrambled (non-recognizable) peptide sequence do not cause enhanced cytotoxicity, demonstrating the enzyme-specific cleavage and subsequent drug release. The unique physicochemical properties, cleavage-dependent cargo release, and tunability of carrier bioactivity by simple peptide exchange highlight the potential of this polymer-nanoparticle concept as platform for custom-designed carrier systems.

1. Introduction

Nanoparticles have proven to be efficient carriers for chemotherapeutics owing to the enhanced permeability of tumor vasculature, resulting in accumulation of nanocarriers in tumor tissues.[1–3] To ensure efficient and selective drug delivery, drug release from the nanocarrier must occur in response to the dysfunctional environment of the tumor or associated vasculature. Over the past decade, intensive research has focused on polymer-peptide conjugates and tumor-targeted drug delivery using carriers that are recognized and cleaved by proteinases.[4–17] Matrix metalloproteinases (MMPs), such as MMP-2, are overexpressed at the invasive front of solid tumors relative to normal tissue and are relatively easy to access by passive accumulation in tissue. By contrast, carriers having reducible or pH-sensitive linkages require transport through cell membranes or diffusion to acidic environments, what might be hard to accomplish.[6–10,18] In comparison to target molecules such as antigens that are overexpressed only in a subset of tumors, MMPs are overexpressed in a variety of tumors, making them a more attractive target for broad-spectrum diagnostic applications.[8,18]

MMP-2 overexpression can be exploited for selective targeting by using carrier systems which contain peptide sequences that are recognized and enzymatically cleaved by the enzyme.[9] Specifically, the selective cleavability of the peptide sequence Pro-Leu-Gly-Leu-Ala-Gly (PLGLAG) recognition site by MMP-2 has been extensively investigated.[7,8,11] For example, Jiang et al. linked two oppositely charged cell-penetrating peptides by an MMP-2 selectively cleavable peptide, in which a payload was attached to the polycationic peptide.[8] Experiments with scrambled peptides as well as experiments where MMP-2 was knocked out demonstrated the selectivity of the PLGLAG sequence toward MMP-2 recognition and cleavage.[8,11] Subsequently, Harris et al. used a similar MMP-2 recognizable peptide as a linker between a hydrophilic polymer and a magneto-fluorescent nanoparticle.[9] In their system, the cell-internalizing domain of the nanoparticle was veiled by the hydrophilic polymer. MMP-2-induced cleavage of the linker caused detachment of the hydrophilic block resulting in selective accumulation of the hydrophobic vehicle in tumor tissues.[9] More recently, this concept was used by Matsumura et al. who similarly linked poly(ethylene glycol) (PEG) to a ferritin nanoparticle via a cleavable peptide (PLGLAG), which carried covalently attached doxorubicin.[19]

Despite the advances toward tumor-targeted carrier systems, challenges remain regarding selective and efficient drug

R. Dorresteijn, Dr. N. Billecke, M. Schwendy, S. Pütz, Prof. M. Bonn, Dr. S. H. Parekh, Dr. M. Klapper, Prof. K. Müllen
Max-Planck-Institut für Polymerforschung
Ackermannweg 10 55128, Mainz, Germany
E-mail: parekh@mpip-mainz.mpg.de; klapper@mpip-mainz.mpg.de

DOI: 10.1002/adfm.201304074

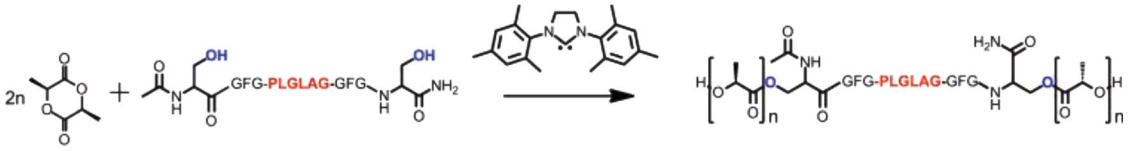

Scheme 1. Reaction scheme of L-lactide polymerization initiated by bioactive peptide.

release. Besides functionality, carrier size is a key issue in efficient drug delivery: a diameter of 100 nm for delivery systems is ideal, being sufficiently small to prevent both recognition by Kupffer cells and drainage into blood capillaries, which is correlated with potential toxicity.[20–22] For delivery systems, which selectively accumulate in tumor tissue after peptide cleavage, aggregation occurs as a consequence of polarity reversal from hydrophilic to hydrophobic.[19] As a result, the carrier size increases,[19] and the carriers can potentially be cleared from the blood stream by Kupffer cells. More importantly, drug release will also be affected by carrier aggregation and resulting local chemical changes, thereby limiting the effectiveness of the strategy. An alternative approach for nanoscale drug delivery is micellar carriers. Micellar carriers are typically less than 40 nm in diameter, which is significantly below the optimal diameter of 100 nm. This small size promotes toxic mechanisms such as redox cycling, and formation of free radicals as well as the aforementioned drainage into blood capillaries.[20–22]

We recently introduced the moisture-sensitive formation of water-stable polylactide-polypeptide triblock copolymers in nonaqueous emulsion (NAE), resulting in poly(L-lactide)-*block*-peptide-*block*-poly(L-lactide) (PLLA-*b*-peptide-*b*-PLLA) triblock copolymer nanoparticles. These particles were readily transferred into an aqueous medium after nonaqueous formation and showed excellent retention of the original 100 nm particle size.[23]

In the current study, we demonstrate the potential of the NAE technique for the generation of carrier systems having defined bioresponsivity by variation of peptide initiator in the ring-opening polymerization (ROP) of lactide. In this way, a bioactive, cleavable peptide is introduced into this system to act as a pre-determined breaking point for triblock copolymer nanocarriers. As the peptide is centered between two PLLA chains, enzymatic cleavage of the triblock copolymer results in bisection of the molecular weight and coincidental reduction of the glass transition temperature (T_g). This physicochemical change of the polymer promotes increased chain mobility, providing a potential pathway for enzyme cleavage-dependent cargo release, without substantially altering particle morphology. Therefore, obstacles concerning encapsulated drug release and the aforementioned aggregation phenomena are not expected here since these nanocarriers remain hydrophilic even after enzyme-triggered cleavage of peptide.

We show MMP-2 cleavage-dependent cargo release and subsequent cellular toxicity, confirming the specificity and utility of these triblock copolymer NAE nanocarriers as potential drug delivery vehicles. The nonaqueous and mild conditions for their preparation permit the usage of temperature- and moisture-sensitive substances, which may not be used in carrier systems originating from aqueous medium such as micellar systems.[24–27] This preparation method therefore substantially broadens the portfolio of permissible compounds for polymerization as well as encapsulation into drug carrier systems.

2. Results and Discussion

2.1. PLLA-*block*-Peptide-*block*-PLLA Copolymer Synthesis and Enzymatic Cleavage

To benefit from physicochemical change of polylactide regarding enhanced cargo release after polymer cleavage, the peptide must be located near the center of a polylactide chain. Hence, a peptide Ac-Ser-Gly-Phe-Gly-Pro-Leu-Gly-Leu-Ala-Gly-Gly-Phe-Gly-Ser-NH_2 (Ac-SGFG-PLGLAG-GFGS-NH_2) was designed, where the two terminal serine units initiate the lactide polymerization, catalyzed by a well-established *N*-heterocyclic carbene,[28,29] and lead to formation of PLLA-*b*-(Ac)SGFG-PLGLAG-GFGS-NH_2-b-PLLA copolymer, carrying a PLGLAG sequence in the center which is cleavable by MMP-2 (**Scheme 1**). Gly and Phe units next to serine constitute spacer groups and allow facile determination of the molecular weight by end-group analysis via ^{1}H NMR spectroscopy.

In order to distinctively assign cleavage of the triblock copolymer to MMP-2 enzyme activity, a comparison specimen having the exact same amino acids, but with a scrambled sequence (LALGPG instead of PLGLAG), was synthesized (**Table 1**). This peptide was previously shown to not be recognized nor cleaved by MMP-2.[8]

PLLA-*b*-(Ac)SGFG-PLGLAG-GFGS(NH_2)-*b*-PLLA copolymers originating from solution polymerization (Sample 1, Table 1) were exposed to MMP-2 for certain periods of time (0.5 h, 2 h, 4 h, 4 days) and subsequently analyzed by MALDI-ToF MS in order to determine the cleavability of the polymer-peptide conjugate. The recognition site (PLGLAG) is known to be cleaved between glycine and leucine.[8,19] Hence, cleavage of peptide should lead to both PLLA-*b*-(Ac)SGFG-PLG-OH and LAG-GFGS(NH_2)-*b*-PLLA copolymers, obviously having different end groups. MALDI-ToF MS measurements of the polymer after exposure to MMP-2 showed cleavage of PLLA-*b*-(Ac)SGFG-PLGLAG-GFGS(NH_2)-*b*-PLLA copolymer. The predicted polymer degradation by MMP-2 was verified by: 1) the decreasing signal-to-noise ratio of the triblock copolymer distribution with MMP-2 incubation time (**Figure 1**, top) and 2) detection of both PLLA-*b*-(Ac)SGFG-PLG-OH and LAG-GFGS(NH_2)-*b*-PLLA with various repeating units (**Figure 2**, top). To assure the assignment of observed signals to "broken" polymers, we compared the obtained signals after degradation with those of the polymer before enzyme incubation (Figure 1 and Figure 2, green).

In contrast to these observations, the matrix-assisted laser desorption/ionization-time-of-flight mass spectrometry (MALDI-ToF MS) spectrum of the polymer bearing a scrambled

Table 1. Experimental conditions and results of the preparation of PLLA-*b*-polypeptide-*b*-PLLA copolymers in solution and nonaqueous emulsion.

Sample	Sequence	M/Cat/I[a)]	M_n[b)] [kDa]	PDI	D_h[c)] (Water) [nm]	D_h[d)] (Serum) [nm]	D_h[e)] (NAE) [nm]	ee[f)] [%]
1[g)]	PLGLAG	17:2:1	2.7	1.17	-	-	-	-
2[h)i)]	PLGLAG	70:2:1	10.0	1.19	98 ± 23	-	92 ± 18	99
3[h)j)]	PLGLAG	70:2:1	8.0	1.07	112 ± 23	176 ± 11	69 ± 3	68
4[g)]	LALGPG	17:2:1	4.7	1.10	-	-	-	-
5[h)i)]	LALGPG	70:2:1	8.0	1.18	107 ± 6	-	106 ± 7	81
6[h)j)]	LALGPG	70:2:1	13.8	1.08	103 ± 14	-	73 ± 5	66

[a)]monomer/catalyst/initiator ratio (n(L-lactide)/n(SIMes)/n(peptide)); [b]number-averaged molecular weight determined via GPC vs. polystyrene standards; [c]hydrodynamic diameter of particles in aqueous dispersion determined via DLS; [d]hydrodynamic diameter of particles in 20 vol% blood serum determined via DLS; [e]hydrodynamic diameter of particles in nonaqueous emulsion determined via DLS; [f]encapsulation efficiency determined via HPLC; [g]solution polymerization; [h]nonaqueous emulsion polymerization; [i]loaded with PMI dye; [j]loaded with 5-fluorouracil.

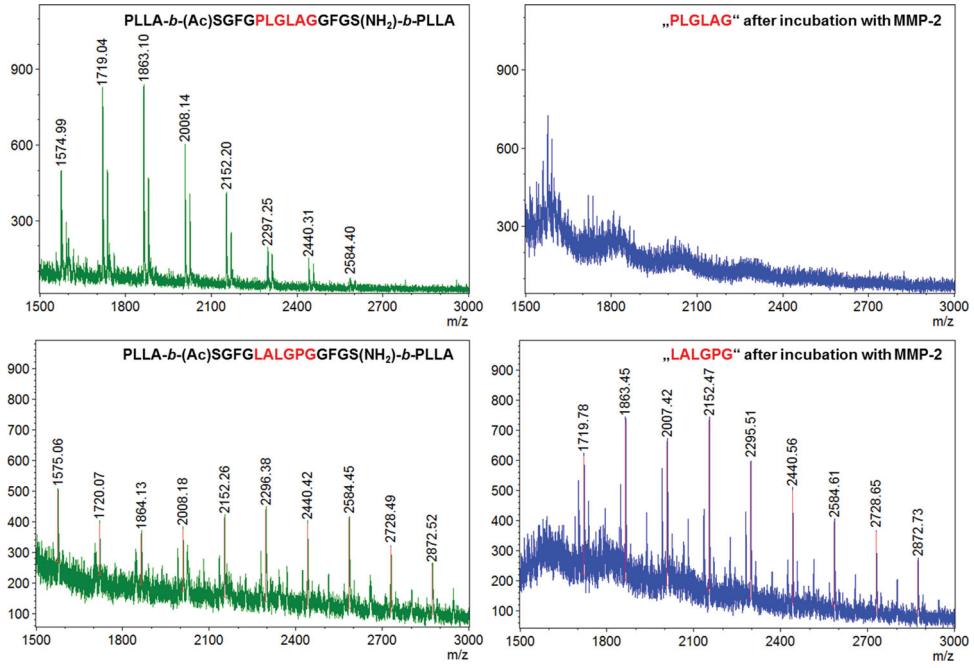

Figure 1. MALDI ToF MS spectra: PLLA-*b*-(Ac)SGFG-PLGLAG-GFGS(NH_2)-*b*-PLLA copolymer sample before (top, green) and after 4 days of incubation with MMP-2 (top, blue); PLLA-*b*-(Ac)SGFG-LALGPG-GFGS(NH_2)-*b*-PLLA copolymer sample before (bottom, green) and after 4 days of incubation with MMP-2 (bottom, blue).

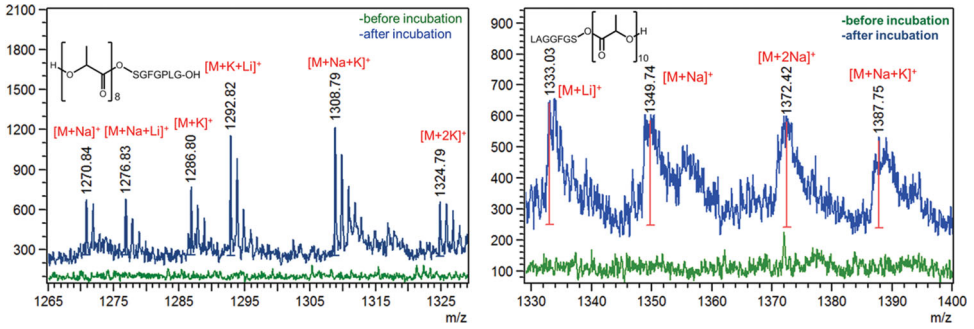

Figure 2. Exemplary PLLA-*b*-(Ac)SGFG-PLG-OH (left) and LAG-GGFGS(NH_2)-*b*-PLLA copolymer fragments (right) before (green) and after 4 days of incubation with MMP-2 (blue).

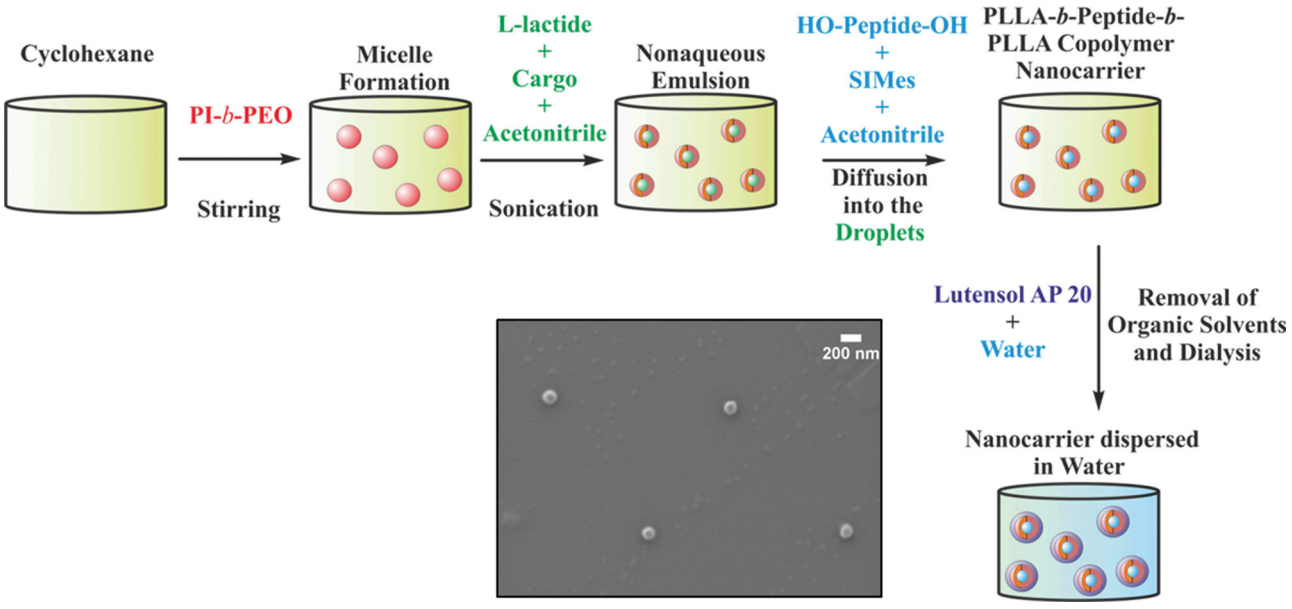

Figure 3. Scheme for preparation of nanoparticles bearing the triblock structure and a typical SEM image of the nanoparticles.

peptide sequence (LALGPG, Sample 4, Table 1) looked identical before and after 4 days of exposure to MMP-2 (Figure 1, bottom). Furthermore, no cleavage products for this scrambled sequence were detected. This clearly demonstrates the enzymatic cleavability of the polymer with the PLGLAG linker peptide.

The observation of the expected copolymer fragments after degradation in MALDI-ToF MS corroborates the presumed hypothesis of peptide incorporation between two PLLA chains. This result is further supported by diffusion ordered NMR spectroscopy (DOSY) measurements showing covalent attachment of peptide and the narrow polydispersity (PDI), strongly suggesting that initiation occurred by initiating groups having equal nucleophilicity.

2.2. Loaded PLLA-*block*-Peptide-*block*-PLLA Nanoparticles in Nonaqueous Emulsion

To impart bioactivity of the polymer for selective drug release from a nanocarrier, we created nanoparticles in nonaqueous emulsion (NAE), wherein acetonitrile was dispersed in cyclohexane and stabilized by a poly(isoprene)-*block*-poly(ethylene oxide) (PI-*b*-PEO) copolymer (DP_{PI} = 441, DP_{PEO} = 357). L-lactide was polymerized in the presence of a cargo molecule (dye or chemotherapeutic agent, Table 1) with either Ac-SGFG-PLGLAG-GFGS-NH_2 or Ac-SGFG-LALGPG-GFGS-NH_2 as initiator resulting in nanoparticles bearing triblock copolymers (Figure 2).

The particles were transferred from the nonaqueous into an aqueous phase and were stabilized with a PEG based surfactant (Lutensol AP20) in order to investigate bioactivity of these nanocarriers. According to dynamic light scattering (DLS) measurements, the particles had an approximate diameter of 100 nm (Table 1), which was similar to that inferred from scanning electron microscopy (SEM) micrographs (**Figure 3**). A monomodal distribution in the DLS measurements provided evidence of well-dispersed, non-aggregated nanocarriers in the aqueous solution. Even in 20 vol% blood serum only a single monomodal peak was observed demonstrating that, on average, no aggregation occurs under physiological conditions. The cargo encapsulation efficiencies (Table 1) exhibited values as high as 99%, as determined by high-performance liquid chromatography (HPLC), demonstrating the high loading capacity of this carrier system.

2.3. Cleavage and Release Studies of Loaded Nanoparticles

2.3.1. Dye-Loaded Nanoparticles

To test for enzymatic specific cleavage of the nanocarrier system and subsequent cargo release, dye-loaded nanoparticles were incubated with MMP-2 for 4 days. After incubation, particle suspensions were centrifuged to pellet the nanocarriers and isolate the released dye from that still contained in the particles. The dye concentration in the supernatant was determined via fluorometry and compared to control samples not incubated with MMP-2. Significantly higher dye release was observed for nanocarriers having an MMP-2 recognition site in the polymer chain (**Figure 4**).

This experiment demonstrates that nanocarriers having the MMP-2 recognition sequence (PLGLAG) in the polymer chain undergo selective cargo release owing to the bioactive polymer constitution of the nanoparticle.

In addition to the fluorometry dye release study, the MMP-2 degraded polymer nanoparticles (containing PLGLAG, sample 3) were further analyzed using gel permeation chromatography (GPC), differential scanning calorimetry (DSC) and DLS. GPC results confirmed that bisection of the original triblock copolymer was accomplished with polymer nanoparticles (Figure S1). DSC measurements of triblock copolymers showed a clear decrease in the glass transition temperature

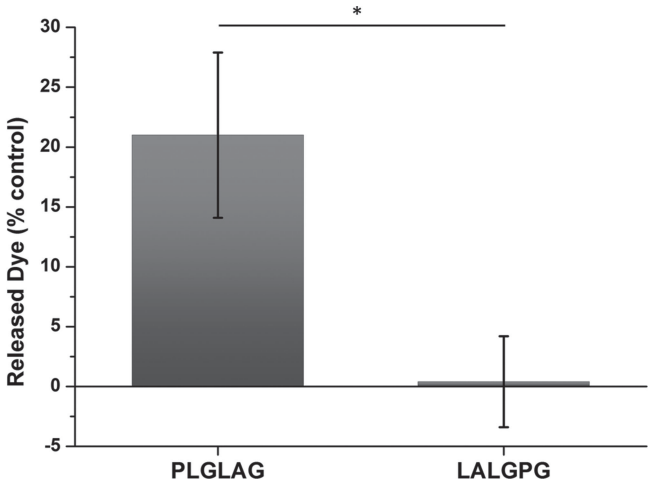

Figure 4. Dye release from nanocarriers bearing either the cleavable sequence (PLGLAG) or the scrambled sequence (LALGPG) in the polymer chain after 4 day incubation time. Each measurement is presented as% released relative to control specimens not incubated with MMP-2. Error bars are standard deviation from three experiments and *marks statistically significant differences between samples with $P < 0.05$.

(T_g) from 39 °C before degradation to 31 °C after degradation (**Figure 5**a). This decrease is expected based on the severing of longer triblock chains into shorter fragments. DLS measurements revealed a slight increase in particle size (~10%) before and after enzymatic cleavage (Figure 5b).

The change in T_g is well-suited for promoting enhanced mobility of cleaved chains within a physiological context to enable diffusion of water molecules into the particles and subsequent cargo release via the concentration gradient. Taken together with the dye release results, these data demonstrate enzymatic cleavage is robust in our NAE particles and suggest a potential cargo-release mechanism based on enhanced polymer chain mobility due to reduced molecular weight after cleavage.

2.3.2. Drug-Loaded Nanoparticles

Based on selective cargo release, we incubated fluorescent PLGLAG-particles with C2C12 cells expressing MMP-2[30] and noted strong interaction between the cells and particles (Figure S2). To determine the applicability of the triblock nanoparticles for specific drug delivery, we synthesized nanocarriers with 5-fluoruracil (5-FU) as the cargo molecule. 5-FU is an extensively investigated chemotherapeutic agent that disrupts RNA transcription and is known to prohibit cell proliferation and cause cell death.[31–33] Both PLGLAG and LALGPG nanocarriers containing 5-FU were synthesized and incubated with C2C12 cells in order to examine cytotoxicity (and specificity) as a response to the bioactive domain (**Figure 6**). Figure 6 shows increased metabolic senescence, decreased cell density, and more pronounced cell death after C2C12 incubation with MMP-2 degradable nanocarriers loaded with 5-FU. The cytotoxic effect of PLGLAG particles was slightly higher than that of free 5-FU (~17%). By comparing this value with the maximum drug content in the particles, calculated from the original sample weight, a high drug release efficiency of greater than 35% within 3 days of incubation was determined. To further verify where the drug molecules are exactly located within the cell after incubation and degradation, it is conceivable to encapsulate molecules which become fluorescent upon activation by specific cell-associated enzymes, as described in previous works.[16]

Incubation of non-degradable nanocarriers with C2C12 cells showed no enhanced cytotoxicity, even at extended times (Figure S3). This experiment demonstrates selective drug release and associated cytotoxicity owing to MMP-2 cleavage of non-leaching defined bioactive polymer-peptide conjugates within the PLGLAG nanocarrier.

3. Conclusion

We have introduced biocompatible, triblock copolymer nanoparticles with enzyme-specific cleavage and tunable functionality. These particles have excellent loading capability that shows targeted drug release in response to MMP-2 enzymatic cleavage. The carrier was generated by ROP of L-lactide with a bioactive, bifunctional peptide initiator in nonaqueous emulsion. The nanoparticles were readily transferred into aqueous medium with 100 nm size retention. The peptide between two PLLA chains acted a predetermined breaking point for the triblock copolymer nanocarriers, which after cleavage by MMP-2 created hydrophilic end groups on each PLLA fragment. The reduced molecular weight of the polymer as well as the end

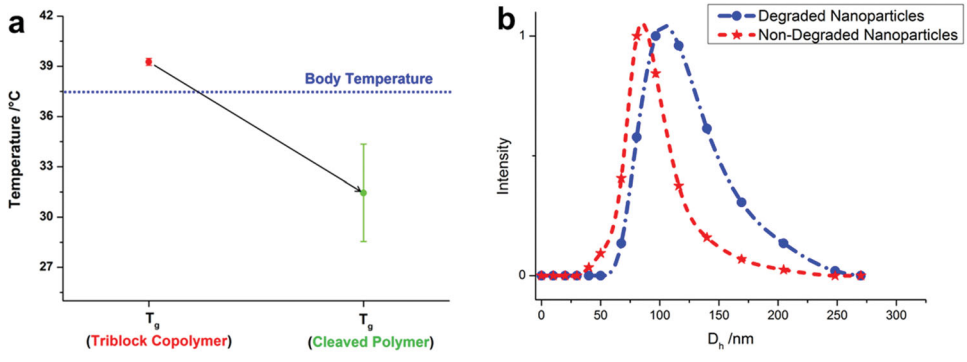

Figure 5. a) Glass transition temperatures of PLGLAG triblock copolymers before (red) and after peptide cleavage (blue) by MMP-2; b) DLS graph of PLGLAG nanoparticles before (non-degraded) and after (degraded) MMP-2 incubation (sample 3, Table 1).

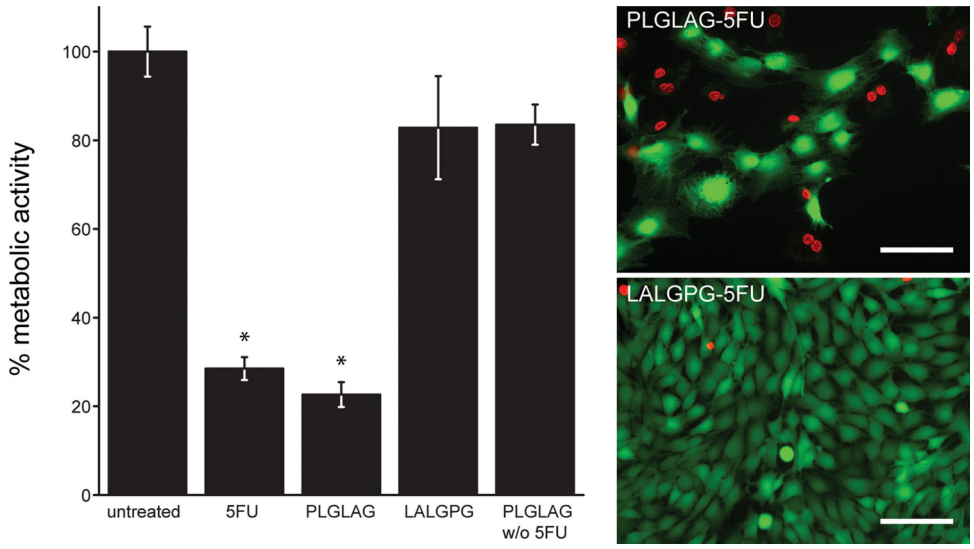

Figure 6. Cytotoxicity by 5-FU-encaspulated nanocarriers bearing the PLGLAG sequence or the LALGPG sequence. Quantitative analysis reveals cytotoxicity for cleavable particles is comparable to soluble 5-FU (10 μg/mL) whereas LALGPG-5-FU and PLGLAG without 5-FU particles show similarly limited toxicity as untreated cells. Images show more living cells retaining calcein-AM (green) and fewer dead cells containing ethidium homodimer (red) in the LALGPG-5FU particles. Error bars are standard deviation from three experiments, *marks statistically significant differences between samples and untreated with $P < 0.05$.

group addition cooperate to reduce the T_g compared to the non-degraded polymer. Under physiological conditions (37 °C), decrease of T_g (to 31 °C) results in higher mobility of the constituent polymers in the particle, which is likely responsible for triggered diffusion of the cargo out of the carrier. This triggered physicochemical change of polymer is most likely imparted to other polyester or even polyurethane systems by using the bifunctional peptide as initiator or co-monomer within this facile method.

Selective cleavage and drug release resulting in cell-death and hampered mitosis was demonstrated by comparing cellular effects using nanocarriers having a scrambled peptide sequence as a linker. Hence, drug release is selectively imparted by polymer cleavage of the carrier with an enzyme overexpressed in tumor tissues, showing that drug release can be tuned with polymer constitution alone. Changing the linking peptide permits custom-designed bioresponsivity, making this a highly promising platform for targeted drug delivery. The current study demonstrates the versatility of our NAE/peptide-initiated polymerization method to construct stable, well-loaded, and selectively-cleavable nanoparticles.

4. Experimental Section

General Remarks: All solvents and reagents were purchased from Sigma Aldrich if not stated otherwise. The poly(isoprene)-*block*-poly(ethylene oxide) (PI-*b*-PEO) copolymer was prepared using a sequential anionic polymerization technique.[34] L-lactide and 1,3-bis(2,4,6-trimethylphenyl)-2-ididazolidinylidene (SIMes) were used as received. SIMes was stored under inert atmosphere at −20 °C. Lutensol AP 20 was obtained from BASF SE in Ludwigshafen. Peptides (Ac-SGFG-PLGLAG-GFGS-NH_2 and Ac-SGFG-LALGPG-GFGS-NH_2) were obtained from Genosphere Biotechnologies in Paris. 9-bromo-*N*-(2,5,8,11,15,18,21,24-octaoxapentacosan-13-yl)perylene-3,4-dicarboxy monoimide (PMI) was prepared according to the literature.[23] To determine the molecular weight and the molecular weight distribution (MWD) of the polylactide-peptide conjugate a gel permeation chromatography (GPC) was carried out at 30 °C using MZ-Gel SDplus 10E6, 10E4 and 500 columns in tetrahydrofuran (THF) as eluent vs. polystyrene standards. The detector was an ERC RI-101 differential refractometer. The composition of the block copolymers was determined by ^{1}HNMR spectroscopy in deuterated dichloromethane (DCM-d2) via peak analysis, using a Bruker Avance III spectrometer operating at 700 MHz. The structure of the polylactide-peptide conjugate was investigated via ^{1}HNMR spectroscopy, diffusion ordered spectroscopy (DOSY) in deuterated dimethylsulfoxide (DMSO-d6) and MALDI-ToF MS. For a ^{1}HNMR spectrum 128 transients were used with an 13.8 μs long 90° pulse and a 12600 Hz spectral width together with a recycling delay of 5 s. The temperature was kept at 298.3 K and regulated by a standard ^{1}H methanol NMR sample using the Topspin 3.1 software (Bruker). The DOSY experiments were done with a 5 mm BBI ^{1}H/X z-gradient probe and a gradient strength of 5.516 [G/mm] on the 700 MHz spectrometer. In this work, the gradient strength was 32 steps from 2% to 100%. The diffusion time d20 was optimized to 80 ms and the gradient length p30 was kept at 1.4 ms. For MALDI-ToF MS measurements the polymer was dissolved in THF and analyzed with alpha-cyano-4-hydroxycinnamic acid as matrix. Scanning electron microscopy (SEM) images were taken using a Zeiss Gemini 912 microscope. The SEM sample preparation proceeded the following way: the nanoparticles were dispersed in cyclohexane and drop casted on a silica wafer. The average diameters of the particles visualized in SEM images were determined by diameter measurements of 100 randomly chosen particles. Dynamic light scattering (DLS) was used to determine the mean size of generated polylactide-peptide nanoparticles (number distribution). The DLS measurements were performed on a Malvern Zetasizer 3000 with a fixed scattering angle of 90° and on an ALV/LSE-5004-correlator using a He/Ne-laser operating at 632.8 nm. The glass transition temperature (T_g) of polymers was determined by peak analysis of differential scanning calorimetry (DSC) graphs using a DSC822e differential scanning calorimeter. The initial temperature of −100 °C was raised to +180 °C with a heating rate of 10 K/min.

Typical Preparation of Poly(L-lactide)-b-polypeptide-b-poly(L-lactide) Copolymer: L-lactide (37.5 mg, 0.26 mmol), SIMes (9.36 mg, 30.6 μmol)

and the peptide (9.30 mg, 7.36 μmol) were dissolved in acetonitrile (0.203 g, 4.94 mmol) and stirred for 15 min at room temperature. After removal of the solvent in vacuo, the triblock copolymer was analyzed with ^{1}H NMR spectroscopy, DOSY, GPC and MALDI-ToF MS.

Typical Preparation of Poly(L-lactide)-b-polypeptide-b-poly(L-lactide) Nanoparticles Loaded with either Dye or Chemotherapeutic Agent: PI-b-PEO copolymer (0.050 g) was magnetically stirred in cyclohexane (14.4 g, 171 mmol) at room temperature. L-lactide (76.0 mg, 0.53 mmol) and PMI (0.30 mg, 0.39 μmol) or 5-fluorouracil (5-FU) (2.6 mg, 0.02 mmol), respectively, were dissolved in acetonitrile (0.230 g, 5.59 mmol). The emulsion was formed by dropwise addition of the monomer/cargo solution to the cyclohexane/PI-b-PEO dispersion and subsequent treatment with sonication for 15 min using a Bandelin Sonorex RK255H ultrasonic bath operating at 640 W. SIMes (9.36 mg, 30.6 μmol) and the peptide (9.30 mg, 7.36 μmol) were dissolved in acetonitrile (0.176 g, 4.29 mmol) and added dropwise to the emulsion under inert atmosphere. The emulsion was stirred for 15 min at room temperature to produce poly(L-lactide)-block-peptide-block-poly(L-lactide) (PLLA-b-peptide-b-PLLA) nanoparticles. A sample was taken out of the emulsion in order to analyze the particle size and morphology via DLS and SEM. 5 ml of the emulsion were precipitated in methanol, separated by centrifugation and dried in vacuo. The polymer was investigated via NMR spectroscopy and via GPC. Furthermore, this solid was dissolved in dioxane and investigated by HPLC analysis in order to determine the encapsulation efficiency.

The remaining emulsion was mixed with a 20 mL of a 0.05 wt% Lutensol AP 20 solution in order to disperse the obtained particles in aqueous medium. The organic solvents were evaporated and the aqueous dispersion was dialyzed against deionized water for 5 days in order to remove unreacted components and organic solvents. Two samples were taken out of the dispersion: one sample was diluted with water and investigated via DLS and SEM to study the morphology. The other sample was dried in vacuo and the resulting solid was analyzed via GPC and NMR spectroscopy. The remaining aqueous dispersion was used for cargo release and cell toxicity studies.

Cleavage Study of the Polymer: PLLA-*b*-peptide-*b*-PLLA copolymer (0.5 mg) was dissolved in 1 mL buffer (100 mM Tris, 10 mM calcium chloride, and 150 mM sodium chloride, pH 8.0). The buffer solution was agitated at 37 °C under 300 revolutions per minute. From a stock solution of MMP-2 (100 μg/mL), 25 μL were incubated with DMSO-solution of APMA (*p*-aminophenylmercuric acetate, 1 mM of APMA) over 2 h at 37 °C under 300 revolutions per minute agitation. After activation, MMP-2 was added to the buffer solution. After certain periods of time (0.5 h, 2 h, 4 h, 4 days) 5 μL of the buffer solution was collected and mixed with 15 μL of CHCA solution (THF) for analysis via MALDI-ToF MS.

Cleavage Study of Particle Dispersions: 250 μL of PMI-loaded particle dispersion was mixed with 250 μL of buffer solution (100 mM Tris, 10 mM calcium chloride, and 150 mM sodium chloride, pH 8.0). From a stock solution of MMP-2 (100 μg/mL in 100 mM Tris, 10 mM calcium chloride, 150 mM sodium chloride, pH 8.0), 15.6 μL was activated with 1mM APMA for 2 h at 37 °C under 300 revolutions per minute agitation. After activation, MMP-2 was added to the particle dispersions in a ratio of 150 μL particles: 250 ng of activated MMP-2. This reaction was incubated in a 300 μL total volume of TCNB buffer (50 mM Tris, 10 mM calcium chloride, 150 mM sodium chloride, pH 7.5) for 4 days at 37 °C under 300 revolutions per minute agitation. Following this incubation, the reaction was centrifuged at 13.4 rpm for 20 min. 200 μL of the supernatant was analyzed via fluorescence spectroscopy in order to determine the concentration of released dye during incubation. Control reactions in which no MMP-2 was used were run in parallel and analyzed in the same way.

Encapsulation Efficiency through High-Pressure Liquid Chromatography (HPLC): The HPLC analysis was carried out with a reversed phase HD C8 column (Macherey-Nagel) using a series 1100 pump (Hewlett Packard). The components, containing in the particles, were detected by a UV-Vis detector S-3702 (Soma). The encapsulation efficiency was calculated by determination of the concentration of either PMI or 5-FU in the solid and its comparison to the applied amount of encapsulated species before the polymerization.

Cellular Interaction Imaging: The interaction of nanoparticles with living cells was done with immortalized C2C12 myogenic cells cultured in chamber slides having coverglass (Thermo Scientific™ Nunc Lab-Tek) bottoms. Cells were allowed to attach to the glass surface and grown to near confluence in growth medium (DMEM low glucose, Gibco) supplemented with 10% fetal bovine serum (Gibco). Directly before imaging, cells were washed 3 times with PBS and PLGLAG particles loaded with the fluorescent dye (9-bromo-*N*-(2,5,8,11,15,18,21,24-octaoxapentacosan-13-yl)perylene-3,4-dicarboxy monoimide, PMI) suspended in growth medium were added. The chambered coverglass was then transferred to a stage-top incubation chamber (Ibidi) mounted on a Leica SP 5 II TCS CARS (Leica Microsystems GmbH) microscope equipped with transmitted and reflected light photomultiplier tubes (PMT). The interior of the incubation chamber was maintained at 37 °C and gassed with ambient air with 5% CO_2. Nanoparticles were detected using laser-based, multiphoton fluorescence in the reflected (epi) PMT while the transmitted PMT was used for forward, label-free coherent anti-Stokes Raman scattering (CARS) microscopy. Briefly, CARS is a multi-photon coherent Raman microscopy that derives contrast from the chemistry of the sample itself without any labels. Using this imaging system, we targeted the CH_2 symmetric vibration in CARS (2845 cm^{-1}) to image the cell borders, intracellular membranes, lipid deposits while imaging the multiphoton fluorescence of PMI in the epi PMT. The excitation source for CARS was two picosecond lasers at 1064 nm and 817 nm (energy difference equal to 2845 cm^{-1}) while multiphoton fluorescence excitation was the 817 nm laser alone (picoEmerald, Angewandte Physik & Eletronik GmbH).

The epi-detection path contained a shortpass filter (750 nm, Chroma Technology) to exclude excitation laser light (and pass PMI two-photon fluorescence) while the forward detection path was equipped with a 750 nm shortpass and additional narrow bandpass filter (660 nm/8 nm bandwidth, Omega Optical) to exclude any two photon fluorescence signal and pass only the CH_2 symmetric CARS signal. Images were acquired every 5 min for 24 h. All images were acquired with a 60X 1.49 NA TIRF objective(Nikon) and subsequently analyzed with ImageJ. Individual time points are shown below (Figure S2).

Cytotoxicity with 5-FU: Cytotoxicity analysis of nanoparticles was done using the immortalized myogenic cell line C2C12. This line has been previously shown to express MMP-2 but not the similar MMP-9.[30] Cells were cultured in growth medium supplemented with 10% fetal bovine serum and grown to ~70% confluence in 96-well plates. To determine particle toxicity, cells were incubated with nanoparticle dispersions bearing either PLGLAG or LALGPG sequence with 5-FU loading (final concentrations of ~8–35 μg/mL) prepared in fresh growth medium. Negative control experiments were done using standard growth medium, and positive control experiments were done using growth medium supplemented with soluble 5-FU at 10 μg/mL. At indicated times, metabolic activity was quantified with standard 3-[4,5-dimethylthiazol-2-yl]-2,5- diphenyltetrazolium bromide (MTT) assays. Briefly, MTT was added directly to each well to a final concentration of 0.7 mg/mL. Cells were then incubated for 3 h at 37 °C. After centrifugation, the supernatant was removed, and the cells were allowed to dry for at least 1h before lysing with 200 μL isopropanol. Formation of formazan crystals was analyzed via the optical density at 560 nm using 670 nm as reference in a spectrophotometer (Tecan). Each experiment was taken out as quintet of wells and repeated three times. Statistical analysis (one-way ANOVA) was performed with Origin 8.5 for Windows, p-Values ≤ 0.05 were considered statistically significant.

Live/Dead Staining: Cells were grown in growth medium in Lab-Tek Chamber Slides (Thermo Scientific Nunc Lab-Tek) to near-confluence similar to cytotoxicity assays. Cells were then incubated for 3 days with PLGLAG or LALGPG nanoparticles with 5-FU loading at a final concentration between 8–35 μg/mL in fresh growth medium. Plain growth medium and medium supplemented with 5 FU (10 mg/mL) served as negative and positive controls, respectively. Following incubation, the medium was exchanged with 2 μM calcein-AM and 4 μM ethidium homodimer (Invitrogen) dissolved in PBS at room temperature. After 30 min of incubation, cells were directly imaged in the

chamber slides on an IX81 inverted microscope (Olympus). Images were collected using the green (excitation BP472/30, emission BP520/35) and red (excitation BP540/20, emission LP590) channels with a 20X, 0.4 NA objective (Olympus). Images were processed with ImageJ.

Supporting Information

Supporting Information is available from the Wiley Online Library or from the author.

Acknowledgements

This work was supported by a Marie Curie Foundation (grant number CIG322284) to S.H.P. We thank Thomas Wagner and Jürgen Thiel for the synthesis of the PI-*b*-PEO copolymer.

Received: December 4, 2013
Revised: January 31, 2014
Published online: March 14, 2014

[1] R. Haag, *Angew. Chem., Int. Ed.* **2004**, *43*, 278–282.
[2] Y. Takakura, M. Hashida, *Crit. Rev. Oncol. Hematol.* **1995**, *18*, 207–231.
[3] F. Yuan, M. Dellian, D. Fukumura, M. Leunig, D. A. Berk, V. P. Torchilin, R. K. Jain, *Cancer Res.* **1995**, *55*, 3752–3756.
[4] J. Andrieu, N. Kotman, M. Maier, V. Mailänder, W. S. L. Strauss, C. K. Weiss, K. Landfester, *Macromol. Rapid Commun.* **2012**, *33*, 248–253.
[5] M. Maier, N. Kotman, C. Friedrichs, J. Andrieu, M. Wagner, R. Graf, W. S. L. Strauss, V. Mailänder, C. K. Weiss, K. Landfester, *Macromolecules* **2011**,*44*, 6258–6267.
[6] Y. Zhang, M. K. So, J. Rao, *Nano Lett.* **2006**, *6*, 1988–1992.
[7] E. S. Olson, T. Jiang, T. A. Aguilera, Q. T. Nguyen, L. G. Ellies, M. Scadeng, R. Y. Tsien, *Proc. Natl. Acad. Sci. USA* **2010**, *107*, 4311–4316.
[8] T. Jiang, E. S. Olson, Q. T. Nguyen, M. Roy, P. A. Jennings, R. Y. Tsien, *Proc. Natl. Acad. Sci. USA* **2004**, *101*, 17867–17872.
[9] T. J. Harris, G. von Maltzahn, M. E. Lord, J.-H. Park, A. Agrawal, D.-H. Min, M. J. Sailor, S. N. Bhatia, *Small* **2008**, *4*, 1307–1312.
[10] C. Bremer, C.-H. Tung, R. Weissleder, *Nat. Med.* **2001**, *7*, 743–478.
[11] E. S. Olson, T. A. Aguilera, T. Jiang, L. G. Ellies, Q. T. Nguyen, E. H. Wong, L. A. Gross, R. Y. Tsien, *Integr. Biol.* **2009**, *1*, 382–393.
[12] G. W. M. Vandermeulen, H.-A. Klok, *Macromol. Biosci.* **2004**, *4*, 383–398.
[13] M. L. Becker, J. Liu, K. L. Wooley, *Biomacromolecules* **2004**, *6*, 220–228.
[14] R. M. Broyer, G. N. Grover, H. D. Maynard, *Chem. Commun.* **2011**, *47*, 2212–2226.
[15] M. L. Becker, J. Liu, K. L. Wooley, *Chem. Commun.* **2003**, 180–181.
[16] P. Rivera-Gil, S. De Koker, B. G. De Geest, W. J. Parak, *Nano Lett.* **2009**, *9*, 4398–4402.
[17] M. Chanana, P. Rivera_Gil, M. A. Correa-Duarte, L. M. Liz-Marzán, W. J. Parak, *Angew. Chem., Int. Ed.* **2013**, *52*, 4179–4183.
[18] Y. Huang, Y. Jiang, H. Wang, J. Wang, M. C. Shin, Y. Byun, H. He, Y. Liang, V. C. Yang, *Adv. Drug Delivery Rev.* **2013**, *65*, 1299–1315.
[19] S. Matsumura, I. Aoki, T. Saga, K. Shiba, *Mol. Pharm.* **2011**, *8*, 1970–1974.
[20] W. E. Bawarski, E. Chidlowsky, D. J. Bharali, S. A. Mousa, *Nanomed.* **2008**, *4*, 273–282.
[21] K. Cho, X. Wang, S. Nie, D. M. Shin, *Clin. Cancer Res.* **2008**, *14*, 1310–1316.
[22] D. F. Emerich, C. G. Thanos, *Biomol. Eng.* **2006**, *23*, 171–184.
[23] R. Dorresteijn, R. Ragg, G. Rago, N. Billecke, M. Bonn, S. H. Parekh, G. Battagliarin, K. Peneva, M. Wagner, M. Klapper, K. Müllen, *Biomacromolecules* **2013**, *14*, 1572–1577.
[24] K. Kazunori, K. Glenn, S. Y. Masayuki, O. Teruo, S. Yasuhisa, *J. Controlled Release* **1993**, *24*, 119–132.
[25] K. Kataoka, A. Harada, Y. Nagasaki, *Adv. Drug Delivery Rev.* **2001**, *47*, 113–131.
[26] R. Duncan, *Nat. Rev. Drug Discovery* **2003**, *2*, 347–360.
[27] H. Bader, H. Ringsdorf, B. Schmidt, *Ang. Makromol. Chem.* **1984**, *123*, 457–485.
[28] S. Csihony, D. A. Culkin, A. C. Sentman, A. P. Dove, R. M. Waymouth, J. L. Hedrick, *J. Am. Chem. Soc.* **2005**, *127*, 9079–9084.
[29] R. Dorresteijn, R. Haschick, M. Klapper, K. Müllen, *Macromol. Chem. Phys.* **2012**, *213*, 1996–2002.
[30] S. Kherif, C. Lafuma, M. Dehaupas, S. Lachkar, J.-G. Fournier, M. Verdière-Sahuqué, M. Fardeau, H. S. Alameddine, *Dev. Biol.* **1999**, *205*, 158–170.
[31] J. Fried, A. G. Perez, J. M. Doblin, B. D. Clarkson, *Cancer Res.* **1981**, *41*, 2627–2632.
[32] P. A. McCarron, A. D. Woolfson, D. F. McCafferty, J. H. Price, H. Sidhu, G. I. Hickey, *Int. J. Pharm.* **1997**, *151*, 69–74.
[33] S. Yamamoto, H. Tanaka, T. Kanamori, M. Nobuhara, M. Namba, *Cancer Lett.* **1983**, *20*, 131–138.
[34] O. Tcherkasskaya, S. Ni, M. A. Winnik, *Macromolecules* **1996**, *29*, 610–616.